

Longitudinal Effects of Asymptomatic *C9orf72* Carriership on Brain Morphology

Kevin van Veenhuijzen, MD ¹, Henk-Jan Westeneng, MD ¹, Harold H. G. Tan, MD ¹,
 Abram D. Nitert, MD ¹, Hannelore K. van der Burgh, PhD ¹, Isabel Gosselt, MSc,^{1,2}
 Michael A. van Es, MD, PhD ¹, Tanja C. W. Nijboer, PhD ³, Jan H. Veldink, MD, PhD ¹
 and Leonard H. van den Berg, MD, PhD ¹

Objective: We investigated effects of *C9orf72* repeat expansion and gene expression on longitudinal cerebral changes before symptom onset.

Methods: We enrolled 79 asymptomatic family members (AFMs) from 9 families with *C9orf72* repeat expansion. Twenty-eight AFMs carried the mutation (C9+). Participants had up to 3 magnetic resonance imaging (MRI) scans, after which we compared motor cortex and motor tracts between C9+ and C9– AFMs using mixed effects models, incorporating kinship to correct for familial relations and lessen effects of other genetic factors. We also compared cortical, subcortical, cerebellar, and connectome structural measurements in a hypothesis-free analysis. We correlated regional *C9orf72* expression in donor brains with the pattern of cortical thinning in C9+ AFMs using meta-regression. For comparison, we included 42 C9+ and 439 C9– patients with amyotrophic lateral sclerosis (ALS) in this analysis.

Results: C9+ AFM motor cortex had less gyrfication and was thinner than in C9– AFMs, without differences in motor tracts. Whole brain analysis revealed thinner cortex and less gyrfication in parietal, occipital, and temporal regions, smaller thalami and right hippocampus, and affected frontotemporal connections. Thinning of bilateral precentral, precuneus, and left superior parietal cortex was faster in C9+ than in C9– AFMs. Higher *C9orf72* expression correlated with thinner cortex in both C9+ AFMs and C9+ ALS patients.

Interpretation: In asymptomatic *C9orf72* repeat expansion carriers, brain MRI reveals widespread features suggestive of impaired neurodevelopment, along with faster decline of motor and parietal cortex than found in normal aging. *C9orf72* expression might play a role in cortical development, and consequently explain the specific brain abnormalities of mutation carriers.

ANN NEUROL 2022;00:1–13

Introduction

Amyotrophic lateral sclerosis (ALS) is characterized by progressive degeneration of upper and lower motor neurons, leading to muscle weakness, respiratory insufficiency and finally death. There is considerable overlap with frontotemporal dementia (FTD); 50% of patients with ALS develop some degree of cognitive or behavioral impairment.¹ In approximately 10 to 20% of ALS cases, a genetic mutation can be identified.¹ The GGGGCC hexanucleotide

repeat expansion (RE) in a noncoding region of *C9orf72* is the most common genetic cause of both ALS and FTD, accounting for approximately 40% of familial ALS, 6 to 10% of sporadic ALS, and 25% of familial FTD in Europe.² Currently, an increasing number of therapeutic options, aimed at specific pathophysiological pathways in *C9orf72*-associated ALS, are being developed.³

Neuroimaging studies in ALS patients carrying *C9orf72* RE consistently report more widespread

View this article online at [wileyonlinelibrary.com](https://onlinelibrary.wiley.com/doi/10.1002/ana.26572). DOI: 10.1002/ana.26572

Received Jul 24, 2022, and in revised form Nov 18, 2022. Accepted for publication Nov 28, 2022.

Address correspondence to Dr van den Berg, Department of Neurology, G03.228, University Medical Center Utrecht, PO Box 85500, 3508 GA Utrecht, The Netherlands. E-mail: l.h.vandenberg@umcutrecht.nl

From the ¹Department of Neurology, Brain Center, University Medical Center Utrecht, Utrecht University, Utrecht, the Netherlands; ²Center of Excellence for Rehabilitation Medicine, Brain Center, University Medical Center Utrecht and De Hoogstraat Rehabilitation, Utrecht, the Netherlands; and ³Department of Experimental Psychology, Utrecht University, Utrecht, the Netherlands

structural cerebral abnormalities compared to ALS patients without this mutation.^{4,5} In a previous cross-sectional neuroimaging study in a family with 16 asymptomatic carriers of *C9orf72* RE, we identified significantly thinner cortex in temporal, parietal, and occipital regions and a lower subcortical gray matter volume compared with asymptomatic noncarriers.⁶ As these (possibly irreversible) impairments are already present at the time of diagnosis, the ability to target *C9orf72*-associated pathophysiological pathways using novel therapies might be limited. The asymptomatic phase might provide an opportunity for early intervention, ideally to a period when neuronal integrity is largely preserved. It is not yet known, however, whether previously identified abnormalities are neurodevelopmental and present from birth, or reflect progressive early neurodegenerative stages of disease in the asymptomatic phase.

To determine longitudinal effects of *C9orf72* RE on the brain prior to symptom onset, we compared gray and white matter structural measurements from repeated magnetic resonance imaging (MRI) scans between asymptomatic carriers and noncarriers of this mutation. As brain morphology is influenced by multiple genetic factors,⁷ we minimized effects of intersubject genetic variation by solely investigating related asymptomatic subjects from families with a family history of ALS. To determine whether gene expression is a mediator of structural brain abnormalities found in *C9orf72* RE carriers, we examined the level of cortical thinning found in mutation carriers in relation to cortical *C9orf72* expression.

Subjects and Methods

Study Participants

This study was approved by the medical-ethical committee of the University Medical Center Utrecht. Written informed consent was obtained from all participants. Between 2010 and

2021, 79 asymptomatic family members (AFMs) of ALS patients from 9 families were included. They were approached by relatives with *C9orf72*-associated ALS, diagnosed at the outpatient clinic for motor neuron diseases of the University Medical Center Utrecht. Individuals were excluded if they were not asymptomatic, or if they had a history of epilepsy, stroke, or structural brain abnormalities. Asymptomatic was defined as absence of signs of upper or lower motor neuron disease, bulbar dysfunction, and behavioral and cognitive changes, during the course of the study and for at least 1 year after the last MRI. All participants underwent a standardized and comprehensive neurological examination at every visit, as described previously.⁸ All examiners regularly operate at our motor neuron disease outpatient clinic and were extensively trained before taking part in our study. Cognitive status of the participants was assessed using the Dutch version of the Edinburgh Cognitive and Behavioral ALS Screen (ECAS), a screening tool to determine cognitive and behavioral changes specific for ALS.⁹ Participants attended the clinic up to 3 times. Follow-up visits were approximately one and a half years (median = 16.9 months, interquartile range [IQR] = 12.8–21.3 months) and 5 years (median = 55.9 months, IQR = 33.7–72.8 months) after the first visit. If family members were to develop possible symptoms of ALS/FTD, they were to report this to our research center and/or visit our motor neuron disease outpatient clinic. At the time of writing, no participant has developed any symptoms within 1 year after the last study follow-up visit.

Additionally, 481 ALS patients were included from a population-based cohort in the analyses correlating brain morphological differences with gene expression, to differentiate between disease effects and effects of carriership of *C9orf72* RE. All patients were diagnosed using the revised El Escorial criteria.¹⁰ The ALS Functional Rating Scale–Revised was evaluated at each visit to determine daily functioning and disease progression rate.¹¹ Clinical data were used from the ongoing PAN (Prospective ALS study the Netherlands).¹²

All subjects were tested for *C9orf72* genetic status by repeat primed polymerase chain reaction in genomic DNA samples as described previously.¹³ Twenty-eight AFMs and 42 ALS patients carried the pathogenic expansion of ≥ 30 GGGGCC

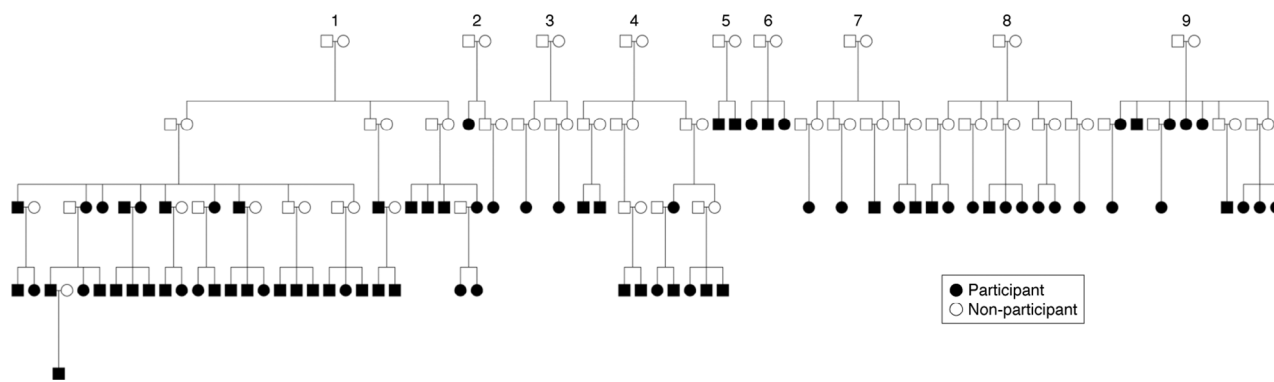


FIGURE 1: Pedigrees of asymptomatic participants with familial amyotrophic lateral sclerosis patients and a *C9orf72* repeat expansion. In these families, 28 participants carry the *C9orf72* repeat expansion. For privacy reasons, we censored this carrier status and only present trimmed pedigrees, omitting nonparticipant members who are not essential for constructing the family tree.

repeats (C9+); 51 AFMs and 439 ALS patients did not (C9−). Only families containing at least one C9+ AFM and one C9− AFM were included in the analyses. The pedigrees of the participating asymptomatic subjects are presented in Figure 1.

MRI Acquisition and Processing

We used a 3T Philips (Best, the Netherlands) Achieva Medical Scanner to acquire T1- and diffusion-weighted images, with imaging parameters and preprocessing as described previously.^{6,14} Cortical and subcortical structures and the cerebellum were processed from T1-weighted images using FreeSurfer v6.0. For cortical parcellation, we used the Desikan–Killiany (DK) atlas.¹⁵ Cerebellar regions were segmented with ACAPULCO (Automatic Cerebellum Anatomical Parcellation using U-Net with Locally Constrained Optimization).¹⁶ In total, 68 cortical, 14 subcortical, 6 ventricular, and 27 cerebellar regions were measured. Longitudinal analysis was performed by creating an unbiased within-subject template space and image using robust inverse consistent registration.¹⁷ Participants with a single scan were also preprocessed using the longitudinal preprocessing stream of FreeSurfer to prevent processing bias.¹⁸ Cortical folding, or gyrification, was measured using the local gyrification index (LGI) as implemented in the FreeSurfer processing pipeline, applying the methods described by Schaer et al.¹⁹ This index quantifies the surface area of cortex buried within the sulcal folds as compared with the area of cortex visible on the outer surface. Extensive folding results in a large LGI, whereas limited folding of cortex gives a small LGI.

White matter tract integrity was assessed from diffusion-weighted images. The images were processed with the TRacts Constrained by UnderLying Anatomy (TRACULA) tool for automated reconstruction of the corticospinal and transcallosal white matter tracts, using global probabilistic tractography.²⁰ The output included average tract fractional anisotropy (FA) and radial diffusivity (RD).

For whole brain connectome analysis, tracts were reconstructed using FACT (Fiber Assignment by Continuous Tracking).²¹ In each white matter voxel, 8 fiber streamlines were initiated and traced from voxel to voxel in the main diffusion direction of each visited voxel, until the stopping conditions described in previous research were met.¹⁴ For each scan, an individual brain network was reconstructed and described as a graph containing a set of nodes and edges linking these nodes. For this set of nodes, 83 segmented brain regions (68 cortical, 14 subcortical, and brainstem), according to the DK atlas, were used. The edges represented the white matter connections between these regions. White matter connectivity strength was measured in FA. The mean FA value of a white matter tract was calculated as the average FA value over all voxels that a streamline traversed, and these mean values were stored in a weighted connectivity matrix. To avoid false positives or spurious fibers, we only considered connections that were present in at least 50% of all C9− AFM subjects.²²

Cortical Gene Expression

The Allen Human Brain Atlas (AHBA) provides a comprehensive library of gene expression in the brain, with complete sample

datasets available at their institute website (<http://human.brain-map.org>). These samples were collected from 6 individuals without history of psychiatric or neuropathological disorders. Gene expression was assayed with custom designed arrays, and samples were mapped to anatomical locations accompanied with Montreal Neurological Institute (MNI) space coordinates. Details of the methods and quality controls are specified in the Microarray Survey Technical White Paper.²³

Expression data obtained in the left hemisphere were available from all 6 donors, but from only 2 donors for the right hemisphere. As such, only the left hemisphere was used for further data analysis. All probes that measure *C9orf72* expression exceeded background noise in >90% of all tissue samples and were, therefore, considered suitable for analysis.²⁴ To address the problem of between-probe inconsistencies, we selected the probe with the most consistent pattern of regional variations across the 6 donor brains, using a measure called differential stability.²⁵

To assign samples to brain regions, French and Paus mapped the MNI coordinates of the cortical tissue samples of the AHBA to the DK atlas and shared this template online.²⁶ As spatial coverage of brain regions varies between donors, we combined samples from all donor brains to form a single atlas with maximum coverage. For this, an appropriate correction for donor-specific transcriptomic probe intensity level patterns is required, as data are collected from people of varying age, ethnicity, sex, medical history, and postmortem interval. We, therefore, applied the scaled robust sigmoid normalization for within-subject probe intensity normalization, which is robust to outliers and ensures equivalent scaling of expression values for each subject in the analysis.²⁷

Neuropsychological Examination

Neuropsychological examination, performed under supervision of a clinical neuropsychologist, was available for a subset of 26 AFMs in our sample. We used the data of this formal neuropsychological assessment to ensure that normal ECAS performance reflected unimpaired neurocognitive status. The examiner was blinded to the subjects' genotype. Visual perception and visuoconstruction were assessed with the Judgment of Line Orientation Task and Rey Complex Figure Test. Executive functions were determined with the Brixton Spatial Anticipation Test. Working memory was examined with the Wechsler Adult Intelligence Scale Digit Span Task and Corsi Block-Tapping Test. Lastly, memory function was assessed with the Rivermead Behavioral Memory Test, Rey Auditory Verbal Learning Test, Rey Complex Figure Test (drawing from memory), and Revised Location Learning Test. For better comparability between tests and groups, all neuropsychological outcome measures were converted into scaled scores, according to the Lezak normal curve score.²⁸ This categorization ranges from 1 to 7 corresponding with percentile scores: 1 (very low) = 0–2nd percentile, 2 (low) = 3rd–9th percentile, 3 (under average) = 10th–24th percentile, 4 (average) = 25th–74th percentile, 5 (above average) = 75th–90th percentile, 6 (high) = 91st–97th percentile, 7 (very high) 98th–100th percentile.

Statistical Analysis

Differences in demographics between groups were calculated using the Mann–Whitney U test for continuous variables and Fisher exact test for categorical variables. To compare neuropsychological performances between groups, we performed ordinal regression analysis using cumulative link models with the scaled assessment outcome as response variable, and age at examination, sex, education level, and *C9orf72* RE carriership as predictors. Upper motor neuron functioning, assessed by physical examination, was also compared between groups. For this, signs most deviant from "normal," either left or right, during any visit, were used. These were compared using either cumulative link models for ordinal data, or binomial logistic regression for dichotomous outcomes. Outcomes of clinical tests were used as response variable; sex, age at examination, and *C9orf72* RE carriership were set as predictors.

As ALS is characterized by deterioration of the primary motor cortex and its associated callosal and corticospinal white matter tracts,¹ we first focused on these parts of the brain with a hypothesis-driven analysis. To give a full appraisal of the effects of *C9orf72* RE on the brain, we also performed a hypothesis-free whole brain analysis comprising cortical thickness, LGI, white matter connectivity, and subcortical, ventricle, and cerebellar volumes.

For the hypothesis-driven analysis, structural brain differences between C9+ and C9– AFMs were compared cross-sectionally and longitudinally. First, we studied group differences by comparing cortical thickness of precentral gyrus and paracentral lobule, and FA and RD of corticospinal tracts and transcallosal motor fibers using linear mixed effects models. As gyrfication during adulthood normally follows a negative logarithmic curve with aging, a nonlinear mixed effects model was used for LGI.²⁹ Age at imaging, sex, and mutation status were included as fixed effects, with total intracranial volume added for LGI analyses. Participant pedigrees were converted to a kinship matrix and used as covariance matrix of random effects to incorporate genetic relationships within the analyzed families, while also nesting by subject ID for modeling the longitudinal measurements. To determine whether cerebral decline through time (ie, aging) is faster or slower in C9+ than in C9– AFMs, we added an age \times mutation status interaction argument to the mixed effects model. Probability values < 0.05 were considered to reflect statistically significant outcomes in these analyses.

For hypothesis-free whole brain analysis, the same mixed effects models were used, with the addition of total intracranial volume as covariable for assessments of subcortical volumes as well. We corrected these analyses for multiple testing by resampling-based familywise error rate correction (10,000 permutations).³⁰ Values of $p < 0.05$ after correction for multiple testing were considered statistically significant. For connectome-based white matter analysis, statistical significance was assessed using Network-Based Statistics (NBS). NBS takes advantage of the property that affected edges in a connectome are more likely to be disease effects when occurring in connected components, instead of in isolation.³¹ Edges were first labeled as affected if the linear mixed effects model resulted in $p < 0.05$. Next, the size of

the largest connected component of these affected connections was tested for significance by comparing it to a simulated null distribution of 10,000 group assignment permutations.

To study the relationship between cerebral *C9orf72* gene expression and the imaging pattern of cortical thinning, as seen in carriership of *C9orf72* RE, we used meta-regression analysis. Cortical thinning was defined as the difference in average cortical thickness between two compared groups, that is, the beta-coefficient of the grouping variable within the previously mentioned mixed effects models. Regional gene expression was computed by calculating the estimated marginal mean of the normalized donor brain probe intensity level with a linear mixed effects model for each DK region, where each donor was added as a random effect. The model was inverse-variance weighted for the standard error of the measurements in each region. To distinguish between disease effect and effect due to mutation, C9+ and C9– ALS patients were also added as groups to these analyses. As such, regional expression in a donor brain was correlated with cortical thinning between (1) C9+ and C9– AFMs, (2) C9+ and C9– ALS patients, and (3) C9+ ALS patients and C9+ AFMs. A p value < 0.05 was considered to reflect a statistically significant result.

Results

Demographics

Demographics and clinical characteristics of the participants are summarized in Table 1. No significant differences were observed for any of the parameters between the C9+ and C9– AFM cohorts. Subjects in the C9+ AFM group were significantly younger than in the C9+ ALS group ($p < 0.001$), and more of them had a higher level of education ($p = 0.032$). Patients in the C9+ ALS cohort were significantly younger than those in the C9– ALS ($p = 0.001$). As there was no direct analysis between the C9– AFM and ALS patient cohorts, their demographics were not statistically compared.

C9orf72 Carriership Group Differences at Physical Examination

No AFMs reported symptoms of dysarthria, dysphagia, muscle weakness, hypertonia, muscle cramps, or problems with mobilization. No clinical signs of lower motor neuron involvement (ie, muscle atrophy, weakness, fasciculations, hyporeflexia) were found at physical examination. Signs that can be associated with mild upper motor neuron involvement were observed in both groups without significant differences between them (Table 2).

Effect of *C9orf72* Carriership on Global Cognitive Functioning

No AFMs reported symptoms of cognitive disturbances during the study, and none showed signs of cognitive impairment on the ECAS. The subgroup of 26 AFMs who underwent full formal neuropsychological examination

TABLE 1. Demographic and Clinical Characteristics of Asymptomatic Family Members and ALS Patients

Characteristic	AFM		ALS	
	C9–	C9+	C9+	C9–
Subjects, n	51	28	42	439
Scans, n				
Visit 1	51	28	42	439
Visit 2	45	28	-	-
Visit 3	4	3	-	-
Follow-up time, mo	18.7 (12.9–22.0)	18.2 (12.9–21.7)	-	-
Sex, male	23 (45.1)	16 (57.1)	28 (66.7)	288 (65.6)
Age at first visit, yr	47.2 (30.3–56.7)	40.8 (30.9–50.8) ^a	57.4 (51.6–63.1) ^{a, b}	63.3 (54.8–68.8) ^b
ISCED 5 or 6	24 (47.1)	16 (57.1) ^a	12 (28.6) ^a	134 (36.3)
Handedness, right	47 (94.0)	24 (85.7)	29 (85.3)	330 (89.4)
Disease duration, mo	-	-	12.3 (3.3–68.3)	14.1 (9.6–22.0)
Bulbar onset	-	-	11 (26.2)	112 (25.5)
ALSFRS-R	-	-	40 (37–44)	40 (36–43)
Disease progression rate	-	-	0.5 (0.3–0.9)	0.5 (0.3–0.8)

Note: Data are shown as median (interquartile range) and count (%). Education level was assessed using the ISCED (1997 version), which was dichotomized into low education (level 0–4) and high education (level 5–6). Disease progression rate was calculated as $(48 - \text{ALSFRS-R})/\text{disease duration}$ (in months).

Abbreviation: AFM = asymptomatic family member; ALS = amyotrophic lateral sclerosis; ALSFRS-R = ALS Functional Rating Scale–Revised; C9– = carriership of *C9orf72* with normal repeat length; C9+ = carriership of *C9orf72* repeat expansion; ISCED = International Standard Classification of Education.

^aSignificant difference between C9+ AFMs and C9+ ALS patients.

^bSignificant difference between C9+ and C9– ALS patients.

consisted of 12 C9+ and 14 C9– AFMs. None of the participants showed impairments on their individual neurocognitive tasks, and there were no significant differences between groups when comparing scores of each task (Table 3).

***C9orf72* Carriership Group Differences in Brain Morphology**

Group differences in brain morphology are presented in Figure 2. Compared to C9– AFMs, we found that C9+ AFMs had significantly thinner right paracentral and bilateral precentral cortex. Although the left paracentral cortex was also shown to be thinner, this difference was not statistically significant. C9+ AFMs had significantly lower LGI in the bilateral precentral and paracentral regions than C9– AFMs. There were no differences in FA or RD of corticospinal and transcallosal motor fibers between groups (data not shown). Whole brain analysis revealed additional cortical and subcortical differences between C9+ and C9– AFMs. Fifteen more cortical regions were

significantly thinner in C9+ AFMs, predominantly situated in the parietal, occipital, and temporal lobes: bilateral superior and inferior parietal, precuneus and lateral occipital, left middle and inferior temporal, supramarginal, cuneus, isthmus of the cingulate gyrus, and right pars opercularis and fusiform regions. Significantly lower LGI was found in C9+ AFMs for the bilateral transverse temporal, left superior temporal, fusiform, parahippocampal, postcentral, superior parietal, pars triangularis, and right pars opercularis, insula, and caudal middle frontal regions. When comparing connectomes, we found a significant component of lower FA in C9+ compared to C9– AFMs (27 connections, $p = 0.023$). This component is mainly situated in the left hemisphere and contains multiple frontotemporal connections. C9+ AFMs had significantly smaller volumes of the thalami and right hippocampus in comparison with C9– AFMs. The left hippocampus showed a similar trend, but this result was not statistically significant after correction for multiple testing. There were

TABLE 2. Outcomes of Physical Examination

Clinical finding	C9– AFMs	C9+ AFMs	p^a	p^b
Dysarthria	0 (0.0)	0 (0.0)	1.00	
Impaired tongue movement	0 (0.0)	0 (0.0)	1.00	
Sustained glabellar reflex	2 (3.9)	1 (3.6)	0.96	
Jaw jerk reflex presence	6 (11.8)	2 (7.1)	0.47	
Snout reflex presence	12 (23.5)	9 (32.1)	0.49	
Palmomental reflex presence	5 (9.8)	3 (10.7)	0.80	
Hypertonia arm muscles	0 (0)	0 (0)	1.00	
Biceps tendon reflex				0.32
Low–normal	38 (74.5)	18 (64.3)		
Brisk	11 (21.6)	9 (32.1)		
Very brisk	2 (3.9)	1 (3.6)		
Triceps tendon reflex				0.19
Low–normal	38 (74.5)	17 (60.7)		
Brisk	11 (21.6)	10 (35.7)		
Very brisk	2 (3.9)	1 (3.6)		
Deltoid tendon reflex presence	5 (9.8)	1 (3.6)	0.31	
Trapezoid tendon reflex presence	5 (9.8)	0 (0.0)	1.00	
Pectoral tendon reflex presence	3 (5.9)	0 (0.0)	1.00	
Hoffmann reflex presence	3 (5.9)	2 (7.1)	0.85	
Abdominal reflex absence	0 (0.0)	0 (0.0)	1.00	
Hypertonia leg muscles	0 (0.0)	0 (0.0)	1.00	
Knee jerk reflex				0.83
Low–normal	34 (66.7)	18 (64.2)		
Brisk	13 (25.5)	10 (35.7)		
Very brisk	4 (7.8)	0 (0.0)		
Ankle jerk reflex				0.90
Low–normal	33 (64.7)	17 (60.7)		
Brisk	10 (19.6)	9 (32.1)		
Very brisk	8 (15.7)	2 (7.1)		
Adductor reflex presence	2 (3.9)	1 (3.6)	0.91	
Plantar reflex Babinski response	0 (0.0)	0 (0.0)	1.00	

Note: Data are shown as count (%). Presence of highest reflex or muscle tone found per subject either left or right across all visits is shown.

Abbreviation: AFM = asymptomatic family member; C9– = carriership of *C9orf72* with normal repeat length; C9+ = carriership of *C9orf72* repeat expansion.

^aProbability value calculated with binomial logistic regression for dichotomous values.

^bProbability value calculated with cumulative link model for ordinal data with 3 levels.

TABLE 3. Outcomes of Neuropsychological Assessment

	C9– AFMs	C9+ AFMs	<i>p</i>
Subgroup demographics			
Subjects, n	14	12	
Age, yr	47.5 (34.5–51.8)	48.5 (41.8–53.5)	0.61
Gender, male	10 (71.4)	6 (50.0)	0.47
ISCED 5 or 6	6 (42.9)	8 (66.7)	0.41
Assessment per cognitive domain			
Executive function			
Brixton spatial anticipation	4 (4–4)	4 (3.75–4)	0.47
Memory			
Direct Rivermead behavioral memory	2 (1–2)	2.5 (2–3)	0.09
Delayed Rivermead behavioral memory	2 (1–3)	3 (1.75–4)	0.22
Direct Rey auditory verbal learning	1 (1–2)	2 (1–2.25)	0.45
Delayed Rey auditory verbal learning	2 (1–3.25)	3 (2.75–3.25)	0.24
Delayed Rey complex figure	4 (2–4)	3 (2–4)	0.86
Location learning	4 (4–5)	4 (4–5)	0.33
Working memory			
WAIS digit span	3 (3–3)	3 (2.75–4)	0.40
Corsi block-tapping	3 (3–4)	3 (3–3)	0.49
Visual perception and visuoconstruction			
Direct Rey complex figure	7 (6–7)	7 (5.75–7)	0.78
Judgment of line orientation	4 (4–5)	4 (4–4.25)	0.89

Note. Data are shown as median (interquartile range) and count (%). Neuropsychological outcome measures were converted, according to Lezak normal curve score, to a 1–7 ordinal scale corresponding with percentile scores: 1 (divergent) = 0–2nd percentile, 2 (low) = 3rd–9th percentile, 3 (below average) = 10th–24th percentile, 4 (average) = 25th–74th percentile, 5 (above average) = 75th–90th percentile, 6 (high) = 91st–97th percentile, 7 (very high) 98th–100th percentile. Probability values for cognitive domain assessments were calculated with cumulative link models.

Abbreviation: AFM = asymptomatic family member; C9– = carriership of *C9orf72* with normal repeat length; C9+ = carriership of *C9orf72* repeat expansion; ISCED = International Standard Classification of Education (1997 version); WAIS = Wechsler Adult Intelligence Scale.

no significant differences in ventricular and cerebellar measurements between groups.

Longitudinal Effect of *C9orf72* Carriership

Longitudinal results are displayed in Figure 3. C9+ AFMs have significantly faster cortical thinning of the precentral cortex over time compared with C9– AFMs. The same trend can be found for the paracentral cortex; this did not, however, reach statistical significance. The slopes of these models, which correspond to yearly rate of cortical thinning, are visualized in Figure 3B. The LGI of the precentral gyrus also declined faster in C9+ than in C9– AFMs, but there were no differences between cohorts for

the paracentral gyrus. There was no accelerated decline of FA or increase of RD in the motor tracts over time in the C9+ AFM cohort compared to C9– AFMs. In whole brain analysis, the precuneus and left superior parietal lobules showed significantly faster cortical thinning over time in C9+ than in C9– after correction for multiple testing. Of note, the subcortical structures with smaller volumes in C9+ AFMs did not show significantly faster volume loss longitudinally (left thalamus, $p = 0.980$; right thalamus, $p = 0.990$; right hippocampus, $p = 0.857$). No additional significant longitudinal differences between cohorts were found when comparing LGI, volumes of the other subcortical gray matter structures, ventricles and cerebellum, or connectomes (data not shown).

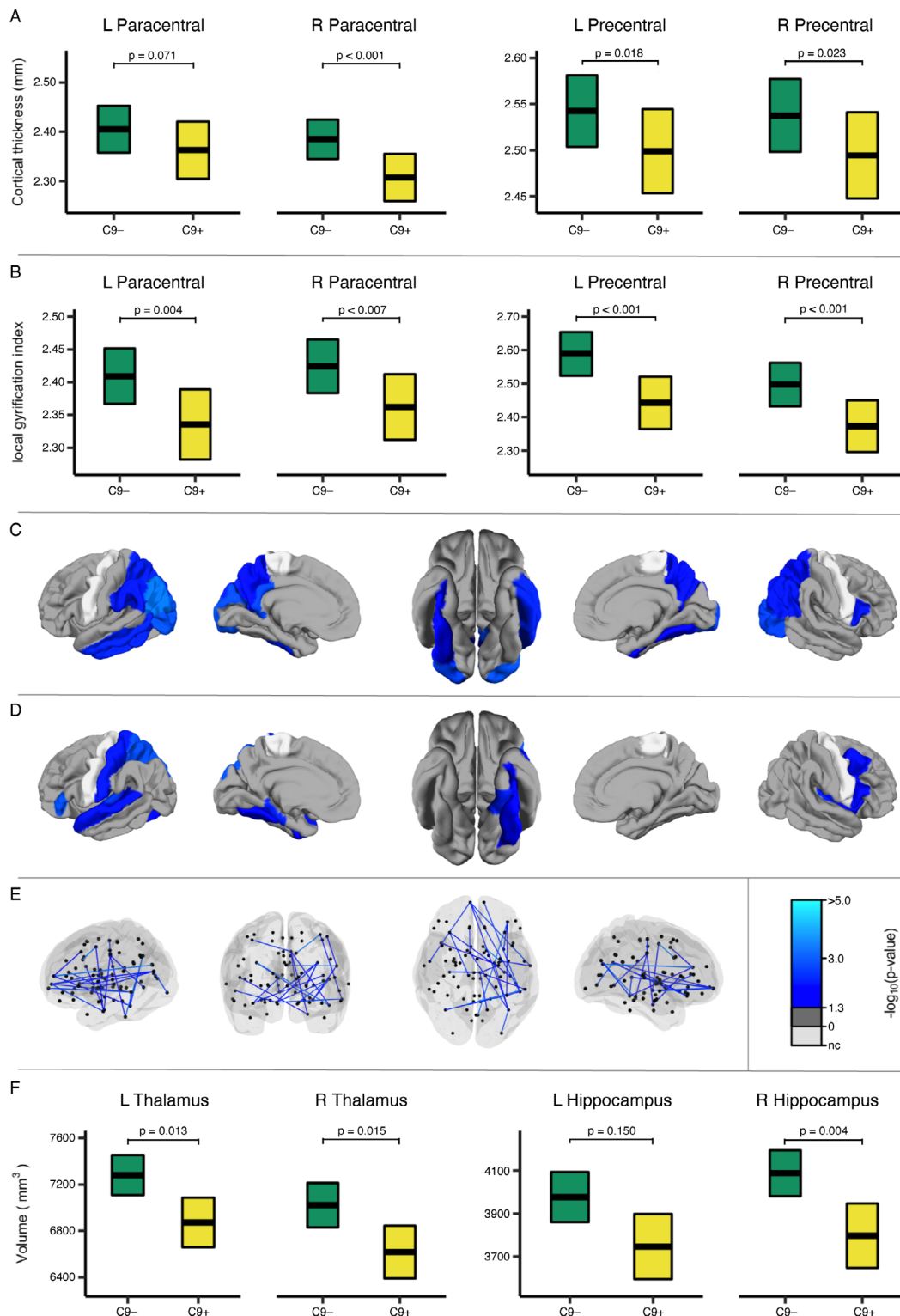


FIGURE 2: Comparing brain structural measurements in asymptomatic family members (AFMs) with (C9+) and without (C9-) *C9orf72* repeat expansion. All measurements were corrected for age, sex, and kinship. Subcortical structure volume measurements were also corrected for intracranial volume. Displayed *p* values for whole brain comparison are after familywise error rate correction. (A) Estimated marginal mean and 95% confidence interval (CI) of motor cortex thickness for C9- and C9+ AFMs. (B) Estimated marginal mean and 95% CI of motor cortex gyrification for C9- and C9+ AFMs. (C) Whole brain comparison of cortical thickness. Significantly thinner regions are marked in blue. Motor cortex is marked in white, as it was not compared (nc) within the hypothesis-free analysis. (D) Whole brain comparison of gyrification indices. Significantly lower gyrification is marked in blue. (E) Whole brain white matter connectome comparison. Significantly affected connections are marked in blue. (F) Estimated marginal mean and 95% CI of subcortical structures with significant differences in volume in hypothesis-free whole brain comparison. For purposes of illustration, the left hippocampus volume is also represented. L = left; R = right.

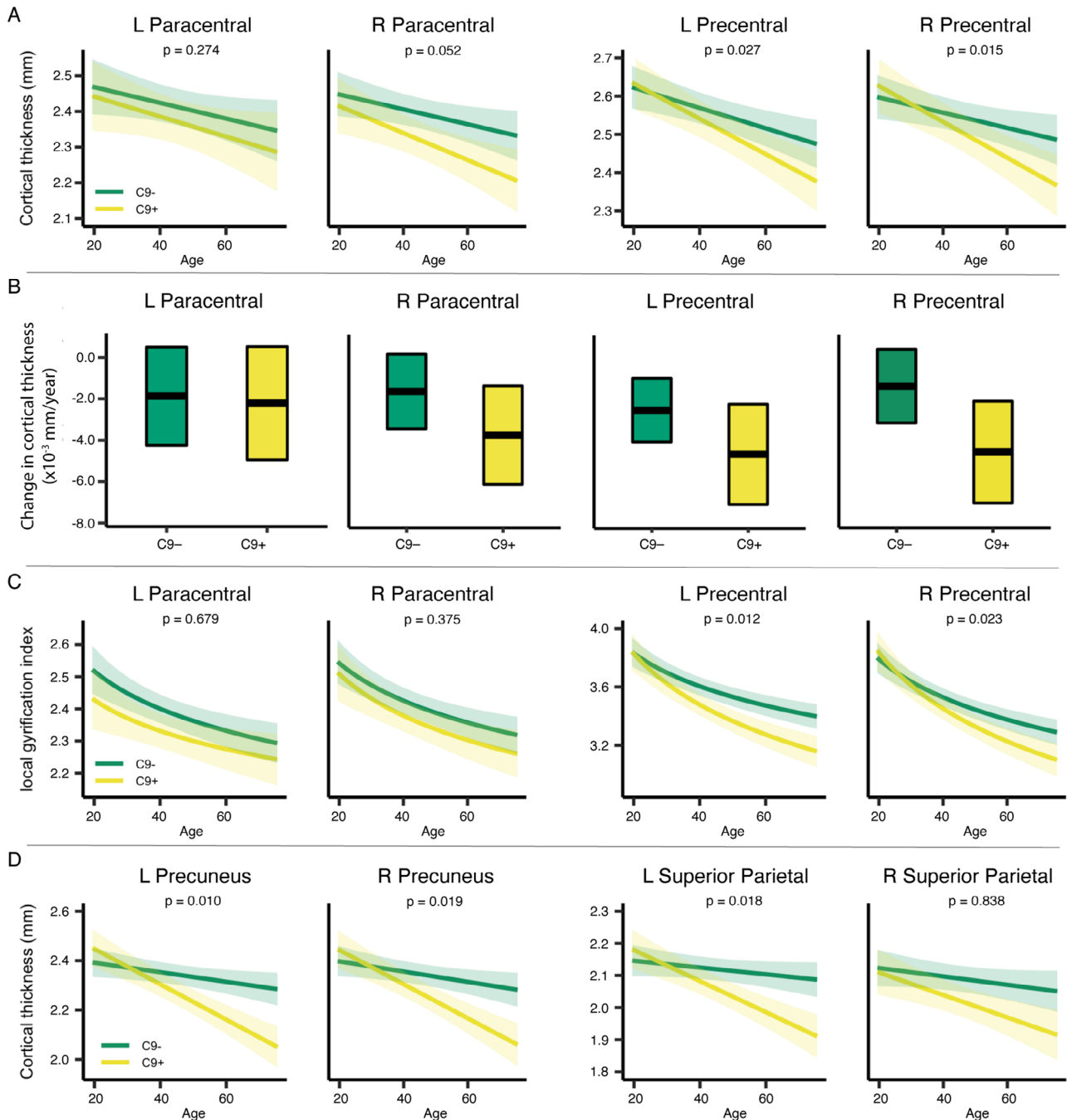


FIGURE 3: Longitudinal trajectories of brain structural measurements between asymptomatic family members with (C9+) and without (C9-) *C9orf72* repeat expansion. All measurements were corrected for age (years), sex, and kinship. (A) Comparison of decline in thickness of motor cortex regions. (B) Visualization of yearly rate of decline in cortical thickness of motor regions per cohort. (C) Comparison of decline in gyrification of motor cortex. (D) Hypothesis-free regionwise whole brain comparison showed the bilateral precuneus and left superior parietal region decline statistically significantly faster in carriers after familywise error rate correction. For purposes of illustration, the right superior parietal region is also represented. L = left; R = right.

Correlation between *C9orf72* Expression and Cortical Thinning

The *C9orf72* transcriptome derived from the donor brains reveals that, on average, there is relatively higher expression of *C9orf72* in the occipital and parietal lobes, and lower expression in the frontotemporal lobes.

Meta-regression of gene expression and cortical thinning shows a negative correlation, where cortical regions with higher *C9orf72* expression in the donor brains are associated with lower cortical thickness in C9+ compared to C9- AFMs (Fig 4). The same significant negative association can be found in ALS patients, where cortical regions

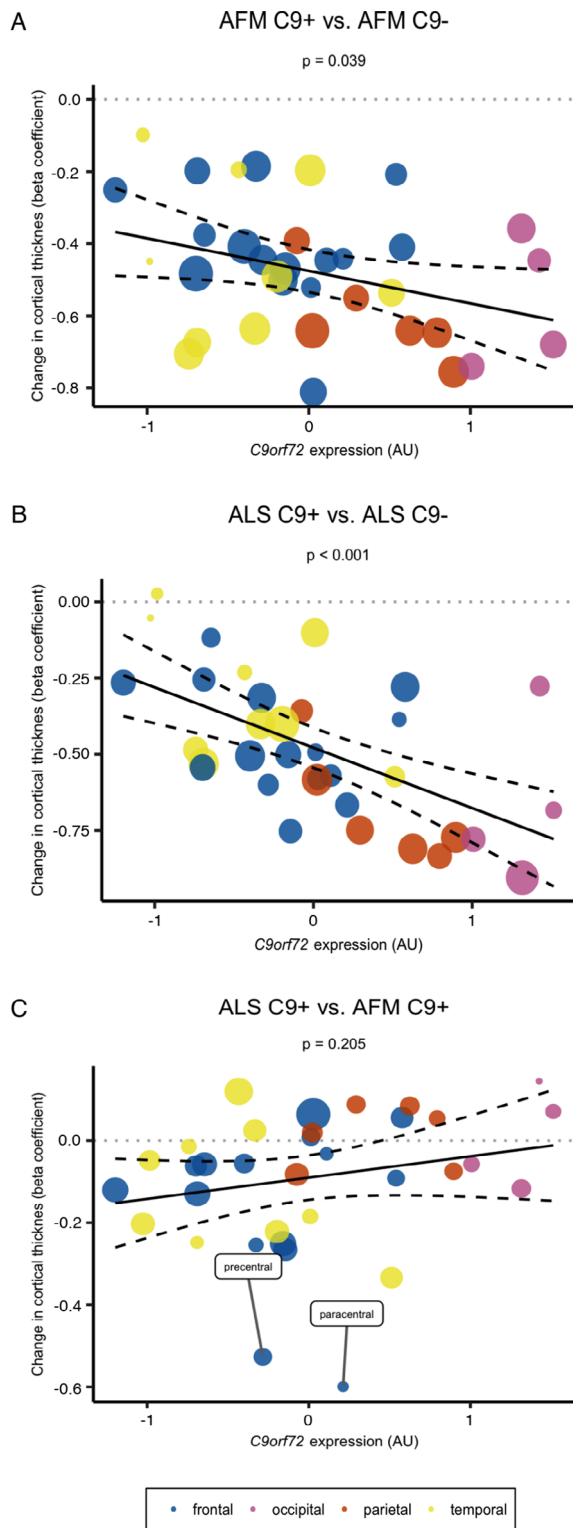


FIGURE 4: Meta-regression correlating average regional *C9orf72* expression and amount of cortical thinning between cohorts. (A) Comparing asymptomatic family members (AFMs) who carry *C9orf72* expansion (C9+) and AFMs who do not (C9-). (B) Comparing C9+ and C9- amyotrophic lateral sclerosis (ALS) patients. (C) Comparing carriers in the ALS and AFM cohorts.

with higher *C9orf72* expression in the donor brains are associated with lower cortical thickness in C9+ compared to C9- ALS patients. When correlating *C9orf72* expression with the difference in cortical thickness between C9+ ALS patients and C9+ AFMs, the association dissipates, leaving the precentral and paracentral gyrus standing out as areas affected by the disease. We found no correlation between regional *C9orf72* expression and rate of cortical thinning in either AFM or ALS subjects (data not shown).

Discussion

We found in asymptomatic carriers that *C9orf72* RE affects brain gyrfication, cortical thickness, subcortical gray matter volume, and white matter connectivity. Longitudinally, asymptomatic carriers had significantly faster thinning of the primary motor cortex and parts of the parietal cortex than seen in normal aging. We identified that cortical regions that normally have the highest *C9orf72* expression are affected the most in mutation carriers. These findings combined suggest that *C9orf72* RE leads to impaired neurodevelopment, as indicated by abnormal gyrfication, affects cortical thickness through *C9orf72* protein expression, and expedites an abnormal decline in specific brain regions, which could predispose to neurodegeneration or be an early stage of neurodegeneration.

In this comprehensive single-center study, we compared 159 scans of related asymptomatic *C9orf72* RE carriers and noncarriers from pedigrees with familial ALS. Brain gyrfication in asymptomatic *C9orf72* RE carriers has not been studied longitudinally before. A previous cross-sectional study (15 carriers, 67 unrelated controls) found 4 small isolated areas with lower gyrfication.³² In our study, we demonstrated widespread lower gyrfication in *C9orf72* RE carriers, involving parts of the frontal, parietal, temporal, and occipital lobe. Gyrfication is a process that begins early in gestation and continues through childhood. Most gyrfication happens during the third trimester of pregnancy, a period in which the brain undergoes considerable development. After peaking during childhood, it declines rapidly during adolescence and early adulthood until it slows down again in later adulthood, following a negative logarithmic curve.²⁹ This decline is thought to be the result of apoptosis and axonal pruning.³³ Abnormal gyrfication, as we have seen in *C9orf72* RE carriers, is thus thought to reflect impaired neurodevelopment.³³ Previous research in animal models has shown that knocking down *C9orf72* gene expression

results in aberrant neural development and cell migration, as well as heightened neuronal apoptosis and overactive microglial pruning.^{34,35} It would be interesting to investigate whether abnormal gyrification in gene carriers is unique to *C9orf72* or also present in other ALS gene carriers, such as the *SOD1* gene, and whether this has implications for the effect of gene therapy in patients. Furthermore, as most changes in gyrification occur early in life, it would be feasible to also include younger participants in future research, to better characterize when these changes start and help define when therapeutic intervention is needed.

We also measured cortical thickness, white matter FA and RD, and volumes of subcortical gray matter, cerebellum, and ventricles. We found that carriers of *C9orf72* RE have thinner motor, temporal, parietal, and occipital cortex, smaller thalami and hippocampus, and impaired frontotemporal white matter connections, without significant differences in the motor tracts or cerebellum. Ten previous studies have analyzed one or more of these modalities in asymptomatic *C9orf72* RE carriers,^{6,32,36–43} of which 3 have a longitudinal design.^{41–43} Between these 3 studies, results are conflicting whether there are baseline differences between carriers and noncarriers, and which regions are involved. Also, in contrast to our study, none of these studies found significant longitudinal differences between carriers and noncarriers. Possible explanations for this difference are smaller sample size in 2 of the 3 longitudinal studies and not including familial controls. As brain morphology is influenced by multiple genetic factors and is partly a heritable trait, it adds the challenge of overcoming the effects of genetic influences other than the gene of interest.⁷ By incorporating kinship in our models, we could lessen these effects and improve statistical power. Lastly, the other large study⁴³ gathered data within a multicenter consortium of 24 research sites with differing MRI scanners, which makes additional correction for confounders necessary and might lead to increased data heterogeneity and thereby less power to detect effects.

The thinner motor and parietal cortex, smaller thalami and impaired frontotemporal white matter in our asymptomatic carriers mirror the phenotype of ALS patients.^{4–6,14} Just like ALS,⁴⁴ asymptomatic carriers selectively showed faster thinning of motor and parietal cortex, which differs from the slow loss of gray and white matter found in normal aging.⁴⁵ This could imply the importance of starting treatment as early as possible, as it appears that a degenerative process is already occurring decades before symptoms would arise. Notably, we found no signs of structural involvement of the corticospinal white matter tracts or transcallosal fibers connected to the motor cortex. As this is considered a hallmark of ALS, the

absence of impairment in asymptomatic carriers highlights them to be disease-defining regions. It would be of interest to follow up asymptomatic subjects for a longer period, to study what happens in the brain around symptom onset, ideally including other (fluid) biomarkers.

With this study, we established a connection between *C9orf72* expression and the pattern of thinner cortex seen in mutation carriers. When we correlated *C9orf72* protein expression with the pattern of cortical atrophy between patients and asymptomatic *C9orf72* RE carriers, the association dissipated, suggesting more an effect of the mutation than a disease effect. No in vivo studies in humans have investigated this before, but this correlation is in line with several studies performed on animal models and human tissue, where multiple downstream effects supporting competing (but nonexclusive) mechanisms were found: loss of expression/function of *C9orf72* protein, and toxic gain of function from *C9orf72* repeat RNA or from dipeptide repeat proteins.⁴⁶ This could explain why the areas that normally have the highest *C9orf72* gene expression are the most vulnerable. We did not, however, find evidence for a connection between *C9orf72* expression and the rate of cortical degeneration in that region. Additionally, we have shown that the motor cortex in ALS patients is much thinner than can be explained by the amount of *C9orf72* expression normally present there. This suggests that other processes than solely a loss or gain of function of *C9orf72* are involved in the pathophysiology of *C9orf72*-associated ALS.

Despite the observed involvement of both motor and extramotor brain regions in carriers of the *C9orf72* RE, no subject reported any symptoms during this study or in the year thereafter. This was also ascertained by repeated extensive physical examinations, performed at our outpatient clinic for neuromuscular diseases, which did not reveal signs of motor neuron disease. Findings that could be associated with mild upper motor neuron involvement (eg, pseudobulbar reflexes and brisk tendon reflexes) were observed equally in both carriers and noncarriers. These mild upper motor neuron signs are known to be observed in healthy subjects as well and do not necessarily indicate pathological changes.⁴⁷ Absence of cognitive dysfunction was determined for all participants by their normal ECAS performances, which has specifically been designed to capture cognitive disturbances distinctive for ALS and has been proven to have both high specificity and sensitivity when measured against formal neuropsychological examination.⁴⁸ Additional comprehensive neuropsychological testing in a sample of participants did not show any sign of dysfunction.

Some limitations of our study should be acknowledged. As our study focused solely on cerebral changes, we

can only draw conclusions regarding upper motor neuron involvement in the brain. Hence, lower motor neuron involvement in our *C9orf72* RE carriers cannot be fully excluded. However, none of the AFMs in our study developed symptoms 1 year after the last visit, making it less likely that lower motor neuron involvement in our subjects had gone unnoticed. As we correlated averaged imaging measurements from our cohort with averaged expression profiles of other postmortem donors, examination of possible individual subject effects is outside the scope of this study. We also had to assume that expression profiles of the donor brains were comparable with those of our living subjects. This method is, however, the best possible option available as it is obviously not feasible or ethical to use tissue from brain biopsies from subjects after they have undergone their MRI scan. The alternative of using future postmortem tissue from our subjects in correlation with neuroimaging performed during their presymptomatic phase would lessen the issue of intersubject variability, but observations regarding gene expression may then be obscured by the presence of end-stage disease effects, and thus would probably not give more insight into the earliest changes than the currently utilized methodology.

Our investigations of asymptomatic *C9orf72* RE carriers further elucidate the role of this mutation in the development of ALS. We found evidence supporting the hypothesis that *C9orf72* RE leads to impaired neurodevelopment, and that *C9orf72* expression could partially explain the pattern of brain atrophy in mutation carriers, suggesting that parts of the brain with higher *C9orf72* expression are more vulnerable to neurodegeneration. This degeneration, which is already apparent in early adulthood, was demonstrated longitudinally with faster cortical thinning in parts of the brain associated with ALS. Our findings could have implications for developing treatment targeting *C9orf72*-related neurodevelopmental abnormalities and ongoing neurodegeneration in *C9orf72* RE carriers.

Acknowledgments

This study received funding from the Netherlands ALS Foundation (Stichting ALS Nederland). This project has received funding from the European Research Council under the European Union's Horizon 2020 research and innovation program (grant agreement 772376–ESCORIAL). Part of this work was supported by HandicapNL (grants R2015010 and R201705758) and seed money grants by Focus Areas DataScience and Research IT from Utrecht University.

We thank all study participants for their valuable time and effort.

Author Contributions

K.v.V., H.J.W., and L.H.B. contributed to the conception and design of the study. K.v.V., H.J.W., H.H.G.T., A.D.N., H.K.v.d.B., I.G., T.C.W.N., M.A.v.E., and J.H.V. contributed to the acquisition and analysis of data. K.v.V., H.J.W., and L.H.v.d.B. contributed to drafting the text or preparing the figures.

Potential Conflicts of Interest

Nothing to report.

References

- van Es MA, Hardiman O, Chio A, et al. Amyotrophic lateral sclerosis. *Lancet* 2017;390:2084–2098.
- Majounie E, Renton AE, Mok K, et al. Frequency of the *C9orf72* hexanucleotide repeat expansion in patients with amyotrophic lateral sclerosis and frontotemporal dementia: a cross-sectional study. *Lancet Neurol* 2012;11:323–330.
- Mayl K, Shaw CE, Lee Y-B. Disease mechanisms and therapeutic approaches in *C9orf72* ALS-FTD. *Biomedicine* 2021;9:601.
- Bede P, Bokde ALW, Byrne S, et al. Multiparametric MRI study of ALS stratified for the *C9orf72* genotype. *Neurology* 2013;81:361–369.
- Westeneng H-J, Walhout R, Straathof M, et al. Widespread structural brain involvement in ALS is not limited to the *C9orf72* repeat expansion. *J Neurol Neurosurg Psychiatry* 2016;87:1354–1360.
- Walhout R, Schmidt R, Westeneng H-J, et al. Brain morphologic changes in asymptomatic *C9orf72* repeat expansion carriers. *Neurology* 2015;85:1780–1788.
- Blokland GAM, de Zubicaray GI, McMahon KL, Wright MJ. Genetic and environmental influences on neuroimaging phenotypes: a meta-analytical perspective on twin imaging studies. *Twin Res Hum Genet* 2012;15:351–371.
- Nitert AD, Tan HHG, Walhout R, et al. Sensitivity of brain MRI and neurological examination for detection of upper motor neurone degeneration in amyotrophic lateral sclerosis. *J Neurol Neurosurg Psychiatry* 2022;93(1):82–92.
- Bakker LA, Schröder CD, Spreij LA. Derivation of norms for the Dutch version of the Edinburgh cognitive and behavioral ALS screen. *Amyotroph Lateral Scler Frontotemporal Degener* 2019;20:19–27.
- Brooks BR, Miller RG, Swash M, et al. El Escorial revisited: revised criteria for the diagnosis of amyotrophic lateral sclerosis. *Amyotroph Lateral Scler Other Motor Neuron Disord* 2000;1:293–299.
- Cedarbaum JM, Stambler N, Malta E, et al. The ALSFRS-R: a revised ALS functional rating scale that incorporates assessments of respiratory function. *J Neurol Sci* 1999;169:13–21.
- Huisman MHB, de Jong SW, van Doormaal PTC, et al. Population based epidemiology of amyotrophic lateral sclerosis using capture-recapture methodology. *J Neurol Neurosurg Psychiatry* 2011;82:1165–1170.
- van Rheenen W, van Blitterswijk M, Huisman MHB, et al. Hexanucleotide repeat expansions in *C9ORF72* in the spectrum of motor neuron diseases. *Neurology* 2012;79:878–882.
- Verstraete E, Veldink JH, Mandl RCW, et al. Impaired structural motor connectome in amyotrophic lateral sclerosis. *PLoS One* 2011;6:e24239.
- Desikan RS, Ségonne F, Fischl B, et al. An automated labeling system for subdividing the human cerebral cortex on MRI scans into gyral based regions of interest. *Neuroimage* 2006;31:968–980.

16. Han S, Carass A, He Y, Prince JL. Automatic cerebellum anatomical parcellation using U-Net with locally constrained optimization. *Neuroimage* 2020;218:116819.
17. Reuter M, Rosas HD, Fischl B. Highly accurate inverse consistent registration: a robust approach. *Neuroimage* 2010;53:1181–1196.
18. Reuter M, Schmansky NJ, Rosas HD, Fischl B. Within-subject template estimation for unbiased longitudinal image analysis. *Neuroimage* 2012;61:1402–1418.
19. Schaer M, Cuadra MB, Schmansky N, et al. How to measure cortical folding from MR images: a step-by-step tutorial to compute local gyrification index. *J Visualized Exp* 2012;59:e3417.
20. Yendiki A, Panneck P, Srinivasan P, et al. Automated probabilistic reconstruction of white-matter pathways in health and disease using an atlas of the underlying anatomy. *Front Neuroinform* 2011;5:23.
21. Mori S, Crain BJ, Chacko VP, van Zijl PC. Three-dimensional tracking of axonal projections in the brain by magnetic resonance imaging. *Ann Neurol* 1999;45:265–269.
22. de Reus MA, van den Heuvel MP. Estimating false positives and negatives in brain networks. *Neuroimage* 2013;70:402–409.
23. Allen T. ALLEN human Brain Atlas Technical White Paper: Microarray Survey [Internet] [cited 2021 Dec 17] Available from: https://help.brain-map.org/download/attachments/2818165/WholeBrainMicroarray_WhitePaper.pdf.
24. Amatkevičiute A, Fulcher BD, Fornito A. A practical guide to linking brain-wide gene expression and neuroimaging data. *Neuroimage* 2019;189:353–367.
25. Hawrylycz M, Miller JA, Menon V, et al. Canonical genetic signatures of the adult human brain. *Nat Neurosci* 2015;18:1832–1844.
26. French L, Paus T. A FreeSurfer view of the cortical transcriptome generated from the Allen human brain atlas. *Front Neurosci* 2015;9:323.
27. Fulcher BD, Little MA, Jones NS. Highly comparative time-series analysis: the empirical structure of time series and their methods. *J R Soc Interface* 2013;10:20130048.
28. Lezak MD, Howieson DB, Bigler ED, Tranel D. *Neuropsychological Assessment*. 5th ed. New York, NY: Oxford University Press, 2012.
29. Cao B, Mwangi B, Passos IC, et al. Lifespan Gyrification trajectories of human brain in healthy individuals and patients with major psychiatric disorders. *Sci Rep* 2017;7:511.
30. Davison AC, Hinkley DV. *Bootstrap methods and their application*. Cambridge, England: Cambridge University Press, 1997.
31. Zalesky A, Fornito A, Bullmore ET. Network-based statistic: identifying differences in brain networks. *Neuroimage* 2010;53:1197–1207.
32. Caverzasi E, Battistella G, Chu SA, et al. Gyrification abnormalities in presymptomatic c9orf72 expansion carriers. *J Neurol Neurosurg Psychiatry* 2019;90:1005–1010.
33. White T, Su S, Schmidt M, et al. The development of gyrification in childhood and adolescence. *Brain Cogn* 2010;72:36–45.
34. Yeh T-H, Liu H-F, Li Y-W, et al. C9orf72 is essential for neurodevelopment and motility mediated by cyclin G1. *Exp Neurol* 2018;304:114–124.
35. Lall D, Lorenzini I, Mota TA, et al. C9orf72 deficiency promotes microglial-mediated synaptic loss in aging and amyloid accumulation. *Neuron* 2021;109:2275–2291.e8.
36. Lee SE, Sias AC, Mandelli ML, et al. Network degeneration and dysfunction in presymptomatic C9ORF72 expansion carriers. *Neuroimage* 2017;14:286–297.
37. Popuri K, Dowds E, Beg MF, et al. Gray matter changes in asymptomatic C9orf72 and GRN mutation carriers. *Neuroimage* 2018;18:591–598.
38. Bertrand A, Wen J, Rinaldi D, et al. Early cognitive, structural, and microstructural changes in presymptomatic C9orf72 carriers younger than 40 years. *JAMA Neurol* 2018;75:236–245.
39. Wen J, Zhang H, Alexander DC, et al. Neurite density is reduced in the presymptomatic phase of C9orf72 disease. *J Neurol Neurosurg Psychiatry* 2019;90:387–394.
40. Bocchetta M, Todd EG, Peakman G, et al. Differential early subcortical involvement in genetic FTD within the GENFI cohort. *Neuroimage* 2021;30:102646.
41. Floeter MK, Bageac D, Danielian LE, et al. Longitudinal imaging in C9orf72 mutation carriers: relationship to phenotype. *Neuroimage* 2016;12:1035–1043.
42. Panman JL, Jiskoot LC, Bouts MJRJ, et al. Gray and white matter changes in presymptomatic genetic frontotemporal dementia: a longitudinal MRI study. *Neurobiol Aging* 2019;76:115–124.
43. Le Blanc G, Jetté Pomerleau V, McCarthy J, et al. Faster cortical thinning and surface area loss in presymptomatic and symptomatic C9orf72 repeat expansion adult carriers. *Ann Neurol* 2020;88:113–122.
44. van der Burgh HK, Westeneng H-J, Walhout R, et al. Multimodal longitudinal study of structural brain involvement in amyotrophic lateral sclerosis. *Neurology* 2020;94:e2592–e2604.
45. Coupé P, Catheline G, Lanuza E, et al. Towards a unified analysis of brain maturation and aging across the entire lifespan: a MRI analysis. *Hum Brain Mapp* 2017;38:5501–5518.
46. Balendra R, Isaacs AM. C9orf72-mediated ALS and FTD: multiple pathways to disease. *Nat Rev Neurol* 2018;14:544–558.
47. Dick JPR. The deep tendon and the abdominal reflexes. *J Neurol Neurosurg Psychiatry* 2003;74:150–153.
48. Niven E, Newton J, Foley J, et al. Validation of the Edinburgh cognitive and behavioural amyotrophic lateral sclerosis screen (ECAS): a cognitive tool for motor disorders. *Amyotroph Lateral Scler Frontotemporal Degener* 2015;16:172–179.